Photosynthesis Research **36**: 43–58, 1993.

Regular paper

Photosynthetic reaction center mutagenesis *via* chimeric rescue of a non-functional *Rhodobacter capsulatus puf* operon with sequences from *Rhodobacter sphaeroides*

Aileen K.W. Taguchi[1], Jonathan W. Stocker[2], Steven G. Boxer[2] & Neal W. Woodbury[1]*
[1]*Department of Chemistry and Biochemistry & the Center for the Study of Early Events in Photosynthesis, Arizona State University, Tempe, AZ 85287-1604, USA*; [2]*Department of Chemistry, Stanford University, Stanford, CA 94305-5080, USA*; **Author for correspondence and reprints*

Received 6 October 1992; accepted in revised form 12 January 1993

Key words: photosynthesis, recombination, bacteria, energy transfer, antenna

Abstract

Photosynthetically active chimeric reaction centers which utilize genetic information from both *Rhodobacter capsulatus* and *Rb. sphaeroides puf* operons were isolated using a novel method termed chimeric rescue. This method involves in vivo recombination repair of a *Rb. capsulatus* host operon harboring a deletion in *pufM* with a non-expressed *Rb. sphaeroides* donor *puf* operon. Following photosynthetic selection, three revertant classes were recovered: 1) those which used *Rb. sphaeroides* donor sequence to repair the *Rb. capsulatus* host operon without modification of *Rb. sphaeroides puf* operon sequences (conversions), 2) those which exchanged sequence between the two operons (inversions), and 3) those which modified plasmid or genomic sequences allowing expression of the *Rb. sphaeroides* donor operon. The distribution of recombination events across the *Rb. capsulatus puf* operon was decidedly non-random and could be the result of the intrinsic recombination systems or could be a reflection of some species-specific, functionally distinct characteristic(s). The minimum region required for chimeric rescue is the D-helix and half of the D/E-interhelix of M. When *puf* operon sequences 3′ of nucleotide M882 are exchanged, significant impairment of excitation trapping is observed. This region includes both the 3′ end of *pufM* and sequences past the end of *pufM*.

Introduction

The membrane-bound proteins which make up the structural framework of the photosynthetic apparatus of *Rhodobacter capsulatus* and *Rhodobacter sphaeroides* are encoded by coordinately regulated operons. Structural genes for the reaction center core subunits as well as the light-harvesting I (LH I or B880) apoproteins are encoded by the *puf* operon. The *puc* operon encodes the light-harvesting II (LH II or B800/850) apoproteins and the *puh* operon encodes a third subunit of the reaction center (Williams et al. 1983, Williams et al. 1984, Youvan et al. 1984, Donohue et al. 1988).

The *puf* operon is the best studied of these operons, both at the level of gene regulation (Scolnik and Marrs 1987, Donohue et al. 1988) and at the level of expressed protein function (Kirmaier and Holten 1987, Feher et al. 1989, Parson 1991). From 5′ to 3′, the *puf* operon is comprised of: *pufQ*, a gene required for bacteriochlorophyll synthesis and/or assembly into the photosynthetic apparatus, *pufβ* and *pufα* which encode the β and α subunits of LH I, *pufL* and *pufM* which are the structural genes

for the L and M subunits of the reaction center, and *pufX* whose specific function is unknown, but which is required for photosynthetic activity. An additional large open reading frame exists further downstream, but it is apparently not required for photosynthetic activity. The homology between most of the genes in the *puf* operons of *Rb. capsulatus* and *Rb. sphaeroides* is high (roughly 70% at the amino acid level for the light-harvesting antenna and reaction center subunits). The three dimensional structure of the *Rb. sphaeroides* reaction center has been determined by X-ray crystallography (Chang et al. 1991, Allen et al. 1987). The similarity between both the primary protein sequences and the kinetic and spectroscopic properties of *Rb. capsulatus* and *Rb. sphaeroides* reaction centers has given rise to the concept that both the overall tertiary structure and the mechanism of electron transfer in the two organisms are very similar. Indeed, it is possible to complement the photosynthetic activity of a *puf* operon deletion in *Rb. capsulatus* with the operon from *Rb. sphaeroides* though the efficiency of energy trapping by the reaction center is apparently significantly impaired (Zilsel et al. 1989).

While conservation of sequence between organisms is usually interpreted in terms of structural motifs that are important in the common mechanistic aspects of function, dissimilarity between sequences is much more ambiguous. It can either indicate that the specific identities of the amino acids under consideration are simply unimportant in the overall function of the system or that those amino acids encode important functional distinctions between species. Thus, the important consideration of mechanistically significant interspecies variation is difficult to recognize or predict by simply analyzing amino acid sequences. Specific mutagenesis could be used to search for such differences, but since prediction is difficult, one immediately confronts the problem of how many mutants must be designed, constructed and screened in order to obtain a representative sample of the species-specific variations.

In this report, a novel method termed chimeric rescue is utilized to generate and isolate strains producing photosynthetically active reaction centers each encoded by a recombinant *Rb. capsulatus* – *Rb. sphaeroides puf* operon. Region-directed in vivo recombination events followed by selection for function are used as a means of identifying and rapidly localizing possible regions with species-specific, functionally important variations in amino acid sequence between the photosynthetic complexes of *Rb. capsulatus* and of *Rb. sphaeroides*.

Materials and methods

Media and bacterial growth

Rhodobacter capsulatus strains were grown at 32 °C aerobically in the dark in MPYe medium (similar to PYS medium, see Bauer et al. 1988, 0.3% (w/v) Bactopeptone, 0.3% (w/v) yeast extract, 1.6 mM $MgCl_2$, 1.0 mM $CaCl_2$) or microaerobically in the dark in RCV^+ medium (Biel and Marrs 1983). RCV is 0.1% (w/v) $(NH_4)_2SO_4$, 0.4% (w/v) DL-malic acid (pH 6.8), 0.5% (v/v) Super Salts, 9.6 mM KPO_4 (pH 6.8). RCV^+ is RCV supplemented with 0.6% (w/v) glucose, 0.5% (w/v) pyruvate, 0.36% (v/v) dimethyl sulfoxide. Super Salts are 0.04% (w/v) disodium ethylenediamine tetraacetate, 0.4% (w/v) $MgSO_4 \cdot 7H_2O$, 0.15% (w/v) $CaCl_2 \cdot 2H_2O$, 2% (v/v) Trace Elements, 0.024% (w/v) $FeSO_4 \cdot 7H_2O$, 0.002% (w/v) thiamine hydrochloride. Trace Elements are 0.16% (w/v) $MnSO_4 \cdot H_2O$, 0.28% (w/v) H_3BO_3, 0.004% (w/v) $Cu(NO_3)_2 \cdot 3H_2O$, 0.024% (w/v) $ZnSO_4 \cdot 7H_2O$, 0.075% (w/v) $NaMoO_4 \cdot 2H_2O$. When appropriate, 15 μg/ml kanamycin (kan) was added to the medium.

Strains and plasmids

Plasmid constructions were carried out in *E. coli* strains DH5α (GIBCO Laboratories-Bethesda Research Laboratories) and S17-1 (Simon et al. 1983), a tra^+ strain. *Rb. capsulatus* strain U43 lacks the reaction center complex as well as both antenna complexes (Youvan et al. 1985). S17-1 transformants were mated to U43 on MPYe plates and replica plated to RCV + kan plates. Transconjugants were streaked to purity on MPYe + kan plates. The plasmids, pU2922 and pU29, were generously provided by Professor D.

Youvan (Youvan et al. 1985, Bylina et al. 1986, Bylina et al. 1989). The plasmids, pCR (*p*lasmid for *c*onjugation and *r*ecombination) and pNJ-1 were constructed from pU2922, pU29, and pBS:ΔM1 as follows. pCR was made from pU2922 by digestion of pU2922 with *Xho*I and *Bam*HI followed by religation. The 0.2 kb *Xho*I–*Xho*I fragment (region 5′ of the major *puf* promoter), the 0.1 kb *Bam*HI–*Xho*I fragment (part of the kan^r cassette), and the 4.0 kb *Bam*HI–*Xho*I fragment (pBR322 sequences including amp^r) were lost, and the 5.7 kb *Xho*I–*Bam*HI fragment containing the *puf* operon was reinserted in an inverted orientation relative to pU2922 (Fig. 1). The growth characteristics and the spectral and biophysical characteristics of U43 transconjugants harboring pCR were identical to those of U43 transconjugants harboring the parental plasmid, pU2922. pNJ-1 (Fig. 2) was constructed by replacing the 3.5 kb *Eco*RI–*Sst*I fragment of pCR with the 3.5 kb *Eco*RI–*Sst*I fragment of pU29:ΔM1, a derivative of pU29 containing the *puf* operon with a 43 bp deletion in *pufM*. pU29:ΔM1 was constructed by replacing the 0.9 kb *Kpn*I–*Bam*HI fragment of pU29 containing the *pufM* gene with the 0.9 kb *Kpn*I–*Bam*HI fragment of pBS:ΔM1. pBS:ΔM1 was constructed by cloning the *Kpn*I–*Bam*HI fragment (*pufM*) of pU29 into the multiple cloning site of Bluescribe (Stratagene) and deleting the region between the *Bst*EII and *Sac*II sites of the *pufM* sequence. The DNA sequence in this region, starting with M665 is 5′-TCCTTGCGGTGACGGGACCGCT-3′ (the fused *Bst*EII–*Sac*II recognition region is underlined). The *Rb. sphaeroides puf* operon was inserted as a *Pst*I fragment lacking the major, oxygen-regulated promoter upstream of *pufQ* (Bauer et al. 1988, Hunter 1991). This 4.5 kb *Pst*I fragment was placed adjacent to the 3′ end of the *Rb. capsulatus puf* operon in an inverted orientation.

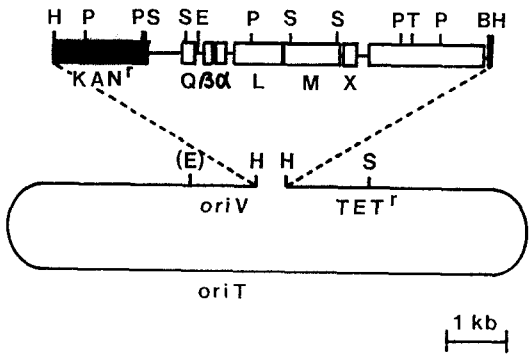

Fig. 1. pCR map. The restriction map of the plasmid for conjugation and recombination is shown. Restriction sites: B, *Bam*HI; E, *Eco*RI; H, *Hin*DIII; P, *Pst*I; S, *Sal*I; T, *Sst*I; (E), *Eco*RI site engineered out. Filled rectangles: kanamycin resistance cassette; open rectangles: *Rb. capsulatus puf* operon genes.

Selection of revertants

Fifty 2 ml cultures of U43 transconjugants containing pNJ-1 were grown from single colonies to stationary phase microaerobically in RCV$^+$ + kan. Cells were harvested and resuspended in 5 ml MPYe + kan. 5 ml of MPYe + kan + 1.5% agar at 48 °C was added to 5 ml of cells in fifty 17 × 100 mm clear polystyrene tubes, mixed gently and allowed to set at room temperature. The tubes were incubated at 32 °C in a home-made temperature-controlled light chamber and illuminated by six 60 W incandescent light bulbs approximately one foot from the tubes. After 3 days, there were 40 ± 30 colonies per tube. One colony from each of 49 tubes was picked, grown photosynthetically in stabs (see below) and incubated in the light chamber. The resulting bacteria were streaked on MPYe + kan plates, a single colony was picked, grown up aerobically in MPYe + kan liquid culture, assayed for photosynthetic growth in stabs (see below), and −80 °C freezer stocks were prepared. These stocks were then used as the source of cells for all future experiments. Forty-four of the original forty-nine revertants retained their ability to grow photosynthetically throughout the purification procedure.

The ability to grow photosynthetically was assayed by stabbing MPYe-grown stationary phase *Rb. capsulatus* strains into 5 ml MPYe + 1% agar in 13 × 100 mm glass culture tubes. Stabs were incubated in the home-made light chamber described above. These simple assays were used to determine whether photosynthetic activity was maintained after either strain manipulation or deletion analysis. For this assay, secondary mutations giving rise to photosynthetic growth could result in false positives if

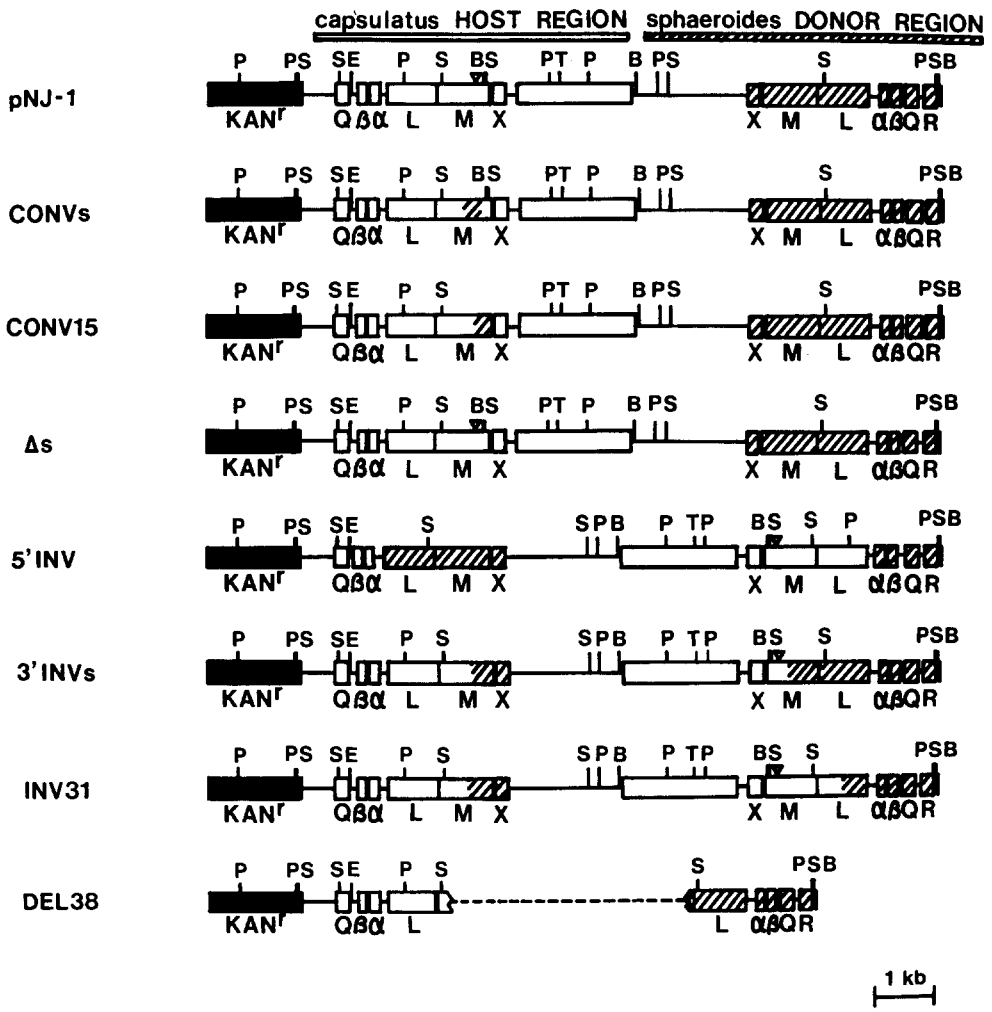

Fig. 2. Plasmid maps. Restriction enzyme maps of the pertinent plasmid section are shown. Each fragment is delineated by *Hin*DIII sites. The delineating and internal *Hin*DIII sites are not shown. Restriction sites and cassettes: see legend to Fig. 1. Hatched rectangles: *Rb. sphaeroides puf* operon genes; dashed line: no restriction sites identified in this region.

the frequency of these events exceeded about 10^{-5}.

Recombinant DNA techniques

General cloning techniques have been described (Maniatis et al. 1982). Direct double-stranded DNA sequencing of the revertant plasmids was carried out using about 20 μg of CsCl-purified DNA (Maniatis et al. 1982) and the Sequenase Version 2.0 DNA Sequencing Kit (US Biochemical Corporation).

Absorbance measurements

Cells grown microaerobically in RCV^+ + kan (also used for time-resolved fluorescence measurements) were diluted with an equal volume of 50 mM KPO_4 (pH 7.35), 50 mM KCl, 40% glycerol and stored at −20 °C. Absorbance spectra of whole cells were taken by adding 25% (w/v) bovine serum albumin (Sigma) to 1.0 ml of cells in order to decrease the scattering background. Measurements were performed with a DU-64 spectrophotometer (Beckman). Alternatively, selected strains were washed with 10 mM

KPO_4 (pH 7.35), sonicated 4 × 10 s on ice, and absorbance spectra were recorded with a Cary5 spectrophotometer (Varian).

Time-resolved fluorescence measurements

Fluorescence decays of whole cells were measured using time-correlated single photon counting. The apparatus has been described previously (Gust et al. 1990, Taguchi et al. 1992). For these measurements, cells were grown microaerobically in RCV^+ + kan and diluted to an optical density of approximately 0.8 (1 cm) at 864 nm in 25 mM KPO_4 (pH 7.35), 25 mM KCl, 20% (v/v) glycerol. Sodium dithionite was added to a final concentration of 10 mM. Samples thus prepared were loaded into a 0.15 cm pathlength fluorescence cuvette. The excitation light levels used were approximately 50 mW/cm^2 at 864 nm and at a repetition rate of 3.8 MHz. Counting rates were 1000–4000 cps. The emission wavelength was 900 nm with a spectral bandwidth of 16 nm. A cooled microchannel plate photomultiplier tube with an S1 photocathode (Hamamatsu) was used as the detector and the overall instrument response function (measured by monitoring the time course of scattered light at the excitation wavelength) was about 80 ps full-width-at-half-maximum.

Results

Chimeric rescue

Plasmid pNJ-1 contains a host *Rb. capsulatus puf* operon with a 43 bp deletion in the *pufM* gene (mutation ΔM1) from nucleotides M678 to M720 and a nonexpressing donor *Rb. sphaeroides puf* operon which contains the structural sequences for genes *pufQ*, *β*, *α*, *L*, *M* and *X* (Fig. 2). This plasmid was transferred from *E. coli* strain S17-1 to *Rb. capsulatus* deletion strain U43 via conjugation. The resulting bacterial strain was incapable of photosynthetic growth, and there was no indication from either the steady-state optical spectrum or the time-resolved fluorescence decay that functional reaction centers were present (see below for details).

These bacteria were placed under selection for photoheterotrophic growth and photosynthetically active recombinants were recovered at a frequency of about 6×10^{-8} on day 3. Forty-nine independent recombinant colonies were picked. After purification, forty-four of these strains were found to grow photosynthetically. Each purified strain was grown heterotrophically in the dark and plasmid was reisolated, transformed into *E. coli* strain S17-1, and prepared for further analysis.

Restriction analysis

Restriction mapping of each plasmid was performed with restriction endonucleases *Sal*I and *Pst*I (Table 1, Fig. 2). The most populous class of mutants (27 mutant plasmids out of 44 total) maintained all of the *Sal*I and *Pst*I sites in both host and donor operons. In this class, the *Sal*I fragment that includes most of the *Rb. capsulatus* donor *pufM* gene was slightly longer than the 0.75 kb fragment found in the parental pNJ-1 plasmid. This indicated that in these isolates the ΔM1 deletion in the *pufM* gene was no longer present in the *Rb. capsulatus* host section. It seemed most likely that information from the *Rb. sphaeroides* donor section had been used to replace some part of the *Rb. capsulatus* host section. No alteration in the restriction map of the adjacent *Rb. sphaeroides* donor section was observed. This class of mutants is the expected result of gene conversion and was designated CONV. Mutant plasmid 15 was also likely to be the result of a conversion event, but in this case the *Sal*I site 3′ of the ΔM1 deletion in the *Rb. capsulatus pufM* gene was lost indicating that the

Table 1. Restriction analysis

Mutant class	No. of members	Plasmids
Parental	1	pNJ-1
CONV	27	4, 7, 11–19, 25, 26, 28, 30, 32–34, 36, 40–42, 44, 45, 47, 49, 50
Δ	11	2, 8, 21, 24, 27, 29, 37, 39, 43, 46, 48
INV	5	1, 5, 22, 31, 35
DEL	1	38

conversion to *Rb. sphaeroides* sequence extended 3′ past this site. This mutant was also placed in the CONV class and was called CONV15.

The next most populous class (11 mutant plasmids out of 44 total) also maintained all the *Sal*I and *Pst*I sites. However, in this case, the *Rb. capsulatus pufM Sal*I fragment was of the size expected for the parental ΔM1 mutation. This class was designated Δ.

Mutant plasmids 1, 5, 22 and 35, all gave restriction patterns indicative of inversions. In these mutants, there had apparently been a single homologous recombination event resulting in replacement of the ΔM1 deletion and all 3′

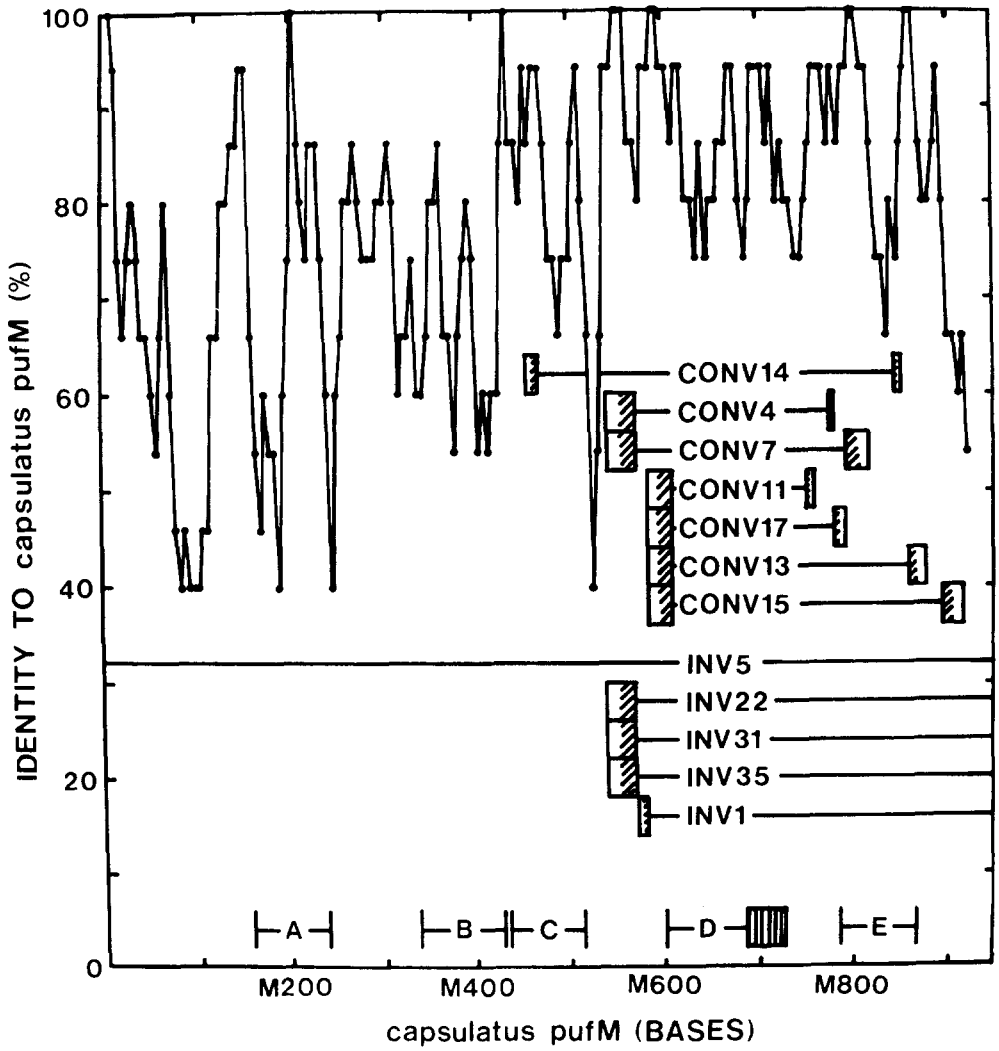

Fig. 3. DNA sequence analysis of the *pufM* gene in the *Rb. capsulatus* donor region. The percentage identity between *Rb. sphaeroides pufM* and *Rb. capsulatus pufM* DNA sequences is shown as a function of location in the *Rb. capsulatus pufM* gene. A moving window of 15 bases was used to calculate an average percentage identity every 5 bases, using a computer program by J. Williams. The x-axis represents the *Rb. capsulatus* host *pufM* coding region. Start and stop codons are not considered. Nucleotide numbering is as in Table 2. The corresponding α-helices in the M protein are shown above the x-axis. The original ΔM1 deletion is represented by a box with vertical stripes. DNA sequencing results from 12 revertants are also shown. Open rectangles: *Rb. capsulatus* gene sequence; hatched rectangles and line: *Rb. sphaeroides* sequence. Precise points at which *Rb. capsulatus* sequence end and *Rb. sphaeroides* sequence begin cannot be determined to the base pair due to the high sequence homology in this region.

sequences in the *Rb. capsulatus* host *puf* operon with *Rb. sphaeroides* donor sequences. This group of mutants was designated the INV class. The inversion point in mutant plasmid INV5 is 5′ to both *Sal*I sites in the *Rb. capsulatus* donor *pufM* and this recombinant was assigned to the 5′INV subclass. The inversion points in mutant plasmids INV1, INV22 and INV35, occur between the two *Sal*I sites in *pufM* and these plasmids were assigned to the 3′INV subclass. Mutant plasmid 31 appears to have arisen through a combination of inversion and gene conversion events. Further phenotypic analysis indicated a similarity to the INVs. It was grouped with the other INVs and called INV31.

Mutant plasmid 38 has undergone a large deletion event removing approximately 2 kb of sequence between the 5′ *Sal*I site of the *Rb. capsulatus* host *pufM* gene and the *Sal*I site of the *Rb. sphaeroides* donor *pufL* gene of the parental plasmid. The *Bam*HI site of the *Rb. capsulatus* host *pufM* gene and the 3′-most *Sal*I site of the *Rb. sphaeroides* donor section were no longer present.

Finally, further restriction analyses of 19 mutant plasmids with one to five enzymes (*Bam*HI, *Eco*RI, *Hin*DIII, *Kpn*I, *Sst*I and *Xho*I) confirmed the above results (Fig. 2).

DNA sequence analysis

DNA sequence analysis was performed on 19 of the mutants. This included eight CONVs which had repaired the original ΔM1 deletion, six Δs which retained the original ΔM1 deletion and all five of the INVs.

Summaries of the results are given in Fig. 3 and Table 2. Sequencing was performed in the relevant region of the *Rb. capsulatus* host *puf* operon and in three cases, also in the *Rb. sphaeroides* donor *puf* operon. As expected from the restriction analysis, sequence analysis of members of the CONV class showed that the original ΔM1 mutation in the *Rb. capsulatus* host *puf* operon had been replaced by wild type *Rb. sphaeroides pufM* gene sequence. These replacement tracts ranged from about 160 bp to about 385 bp in length. The endpoints of the conversions tracts could not be assigned to specific nucleotides due to the high degree of identity (≥80%) between the *Rb. capsulatus* and *Rb. sphaeroides pufM* genes in this region. All three CONV mutants (CONV7, CONV17, CONV18) that were sequenced in the *Rb. sphaeroides* donor *puf* operon showed wild type *Rb. sphaeroides* sequence in the region of *pufM* that had presumably been used to repair the *Rb. capsulatus pufM* deletion.

Sequence analysis also verified the presence of

Table 2. DNA sequence analysis[a]

Conversion tracts			Inversion points	
Mutant	5′ End[b]	3′ End[c]	Mutant	INV point[b]
CONV4	M528–M559	M762–M768	INV1	M561–M572
CONV7	M528–M559	M780–M804	INV5	*pufβ*, *pufα*[d]
CONV11	M572–M597	M738–M747	INV22	M528–M559
CONV13	M572–M597	M846–M864	INV31	M528–M559
CONV14	M444–M456	M831–M837	INV35	M528–M559
CONV15	M572–M597	M882–M890		
CONV16	–	M780–M804		
CONV17	M572–M597	M768–M780		

[a] Base M4 is the first base (G) of the second codon (GCT) which codes for the first amino acid (ala) of the active M protein.
[b] The first base of the indicated range is the last *Rb. capsulatus* base identified where a non-identity exists between the two species and the last base is the first *Rb. sphaeroides* base identified.
[c] The first base of the indicated range is the last *Rb. sphaeroides* base identified and the last base is the first *Rb. capsulatus* base identified.
[d] The inversion point in INV5 is located in the 0.5 kb *Eco*RI–*Hin*DIII fragment which roughly delineates the *pufβ* and *pufα* genes of *Rb. capsulatus*.

the ΔM1 deletion in five revertant plasmids of the Δ class. In fact, sequence analysis in that region of the *pufM* genes from both the *Rb. capsulatus* host and *Rb. sphaeroides* donor *puf* operons detected no changes from the parent plasmid, pNJ-1. Apparently, this type of reversion involves changes elsewhere in the plasmid or in the *Rb. capsulatus* genome.

Sequencing of the five INV mutants indicated that the inversion points for four of the mutants were located between M528 and M572 in the *Rb. capsulatus puf* operon and presumably, near the corresponding sites in the *Rb. sphaeroides* operon (not sequenced). However, the inversion point for INV5 was located near *pufβ/α* (not sequenced) in the *Rb. capsulatus puf* operon.

Plasmid-dependence of the photosynthetic phenotype

To ascertain whether the photosynthetically active phenotype was due to a plasmid-based alteration or to a genomic alteration, 18 of the sequenced plasmids were mated into the original plasmid-less, *Rb. capsulatus* deletion strain, U43. The seven newly mated CONVs (CONV4, CONV7, CONV11, CONV13, CONV14, CONV15, CONV17) and the five newly mated INVs (INV1, INV5, INV22, INV31, INV35) were all photosynthetically active. In addition, half of the newly mated Δs (Δ2, Δ8, Δ27) were photosynthetically viable. These Δ plasmids were assigned to the Δ_p subclass. The three remaining Δ revertant plasmids (Δ21, Δ24, Δ29) did not confer photosynthetic activity on U43, indicating that a mutation not on the plasmid isolated from the original revertant strains contributed to the recovery of photosynthetic activity. We assigned these plasmids to the Δ_o subclass.

The Δ_o subclass was further analyzed by curing the original revertant strains of plasmid (Magnin et al. 1987) and recomplementing these cured strains with either pCR or pNJ-1. All of the cured Δ_o strains were able to be complemented with pCR, yielding vigorous photosynthetic growth, but were not complemented for photosynthetic ability with pNJ-1. This indicates that the reversion event was not entirely due to either the plasmid isolated from these strains or the genome. Either additional plasmids or interactions between the plasmid sequences and genomic sequences were presumably involved in the restoration of photosynthetic growth in the Δ_o subclass.

Deletion analysis

Deletion analysis was used to determine which of the two *puf* operon sequences on the plasmid were sufficient for photosynthetic activity in the Δ, CONV and the INV revertant classes. The three Δ_p revertant plasmids (Δ2, Δ8, Δ27) were examined by deletion analysis. Plasmids of this subclass were not likely to require the *Rb. capsulatus* host section for photosynthetic activity due to the presence of the original ΔM1 mutation. The *Rb. capsulatus* host section was deleted as an *Eco*RI–*Sst*I fragment (E-T in Fig. 2), and the plasmids were treated with mung bean nuclease and religated. The Δ_p revertants were photosynthetically viable when *Rb. capsulatus* host sequences (*pufβ*, *α*, *L*, *M* and *X*) were removed.

Similarly, the five INV plasmids (INV1, INV5, INV22, INV31, INV35) and one of the CONV plasmids (CONV15) were examined following deletion of the *Rb. sphaeroides* donor section as a *Bam*HI fragment. All of the INV and CONV revertants tested involving repair of the deletion in the *Rb. capsulatus pufM* gene did not require *Rb. sphaeroides* donor sequences to maintain photosynthetic activity.

In addition to photosynthetic growth characteristics, absorbance spectra and fluorescence decay kinetics were also recorded for each of the deletion strains. There was no significant change in any of these phenotypic parameters for deletion transconjugants of the INV, CONV or Δ_p subclasses when compared to the original revertant strains. This indicates that the phenotype of each of these revertants is due to the observed changes in the plasmid-borne *puf* operon of *Rb. capsulatus* (CONV and INV subclasses) or *Rb. sphaeroides* (Δ_p subclass). This is in contrast to the results for the Δ_o subclass described above.

Absorbance spectra

Spectra of whole cells were taken for all forty-four revertant strains, and the results were

consistent for each type of reversion event. Figure 4 shows several representative spectra of sonicated cells. The wild type strain containing pU2922 (Fig. 4A) shows the highest absorbance among all the strains examined both at 880 nm, the primary absorbance peak of the B880 antenna, and at 800 nm, a reaction center absorbance peak. In contrast, the primary antenna band (880 nm) of the parental strain containing pNJ-1 is reduced by as much as 10-fold relative to wild type and little if any of the 800 nm band is seen (Fig. 4F). Both the INV revertants (Fig. 4B) as well as the CONV revertants which involved replacement of a small section of *Rb. capsulatus* sequence with *Rb. sphaeroides* sequence (Fig. 4C) have qualitatively wild type-like spectra. However, there is a roughly 2-fold reduction in the amount of antenna absorbance at 880 nm. In the Δ_o and Δ_p revertants which still maintained the original ΔM1 mutation (Fig. 4D, 4E), the antenna absorbance is decreased relative to wild type by about 3-fold.

*Bam*HI deletions of *Rb. sphaeroides puf* operon did not significantly alter the spectra of either the CONVs or INVs. In addition, the

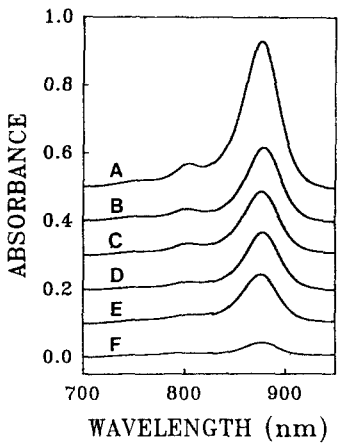

Fig. 4. Absorbance spectra of sonicated cells. Absorbance spectra of sonicated cells were recorded with a Cary5 spectrophotometer. Spectra were normalized at 700 nm. A scattering curve was generated by measuring the spectrum of deletion strain U43 without a plasmid and was subtracted from the spectra. The spectra were then displaced from each other by 0.1 absorbance units for clarity. The plasmids were A: pU2922 (wild type), B: INV1 (3'INV), C: CONV4, D: Δ21 (Δ_o), E: Δ2 (Δ_p), F: pNJ-1 (parent).

*Eco*RI–*Sst*I deletions of the *Rb. capsulatus puf* operons from the Δ_p revertants yielded spectra in agreement with those of the original Δ_p revertants.

Time-resolved single photon counting measurements

In order to investigate energy and electron transfer in these mutants, a series of time-resolved fluorescence decay measurements were performed on whole cells. Essentially all of the fluorescence observed in such a measurement is emitted from the excited singlet state of the B880 antenna (LH I). Thus, these measurements are sensitive to processes which quench that fluorescence, such as electron transfer in the reaction center (van Grondelle 1985, Woodbury and Parson 1986, Valkunas et al. 1991).

The fluorescence decay from wild type whole cells is essentially identical to that seen previously from isolated membranes considering the decreased timescale and increased time resolution of data collection (Woodbury and Parson 1986, Fig. 5A, Table 3). Most of the fluorescence (98%) decays in less than 50 ps and a small amount of a long-lived (about 6 ns) component is present which is thought to represent the product of charge separation when electron transfer to the quinone is blocked (Woodbury and Parson 1986). The CONV revertants in which the ΔM1 deletion of *pufM* in the *Rb. capsulatus* operon was replaced by a section of *Rb. sphaeroides pufM* had fluorescence decay time courses that are essentially identical to wild type (Fig. 5C, Table 3). The fluorescence decay from all of the other revertants was slower, dominated by a 74–106 ps component (τ_1), and showed a substantial relative increase in the 500–900 ps fluorescence decay component (τ_2) (Fig. 5B, 5D, 5E and Table 3). This indicated less efficient overall excitation trapping in these mutants. In all of the revertants and wild type (but not in pNJ-1) roughly 1% of the fluorescence decay occurred on a 5–6 ns timescale, indicating a substantial yield of charge separated product. In the photosynthetically inactive parental strain containing pNJ-1, 90% of the fluorescence decayed on the 500–900 ps timescale (τ_2), and the 300 ps com-

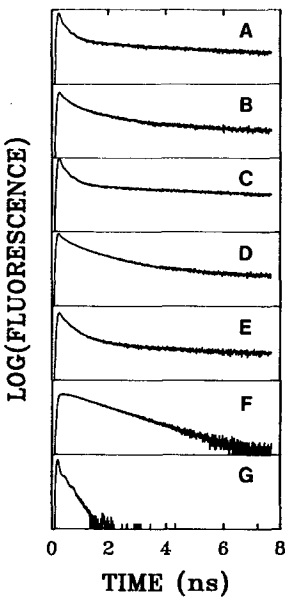

Fig. 5. Time-correlated single photon counting traces of whole cells under reducing conditions. The secondary electron acceptors in the reaction center, the quinones, were reduced by addition of 10 mM dithionite to prevent build-up of the long-lived state $P^+Q_A^-$ and to facilitate detection of long-lived fluorescence due to back electron transfer from $P^+Bph_A^-$ in the reaction center. Sample conditions were as described in methods. Each trace was normalized at the peak fluorescence value. Samples A through F are as in the legend to Fig. 4. G is an instrument response function generated by measuring the time course of scattering at the excitation wavelength.

ponent (τ_1) was only a small fraction of the total initial fluorescence amplitude (Fig. 5F, Table 3). The pNJ-1 containing strain showed no fast ($\leq$100 ps) phase (τ_1) and no 5–6 ns phase (τ_3).

The Δ_p (Δ2, Δ8, Δ27) and Δ_o (Δ21, Δ24, Δ29) subclasses identified on the basis of plasmid-dependence of photosynthetic activity displayed distinguishable fluorescence phenotypes; the Δ_o subclass exhibited much less efficient antenna fluorescence quenching than the Δ_p subclass with about half of the fluorescence decay occurring on the nanosecond timescale (τ_2). This phenotype was used to assign the remaining Δ mutants for which deletion analysis was not performed (Δ37, Δ39, Δ43, Δ46, Δ48) to the Δ_o subclass.

Strains containing the deletions constructed from the CONV, INV and Δ_p plasmids were also subjected to single photon counting. These strains yielded fluorescence phenotypes indistinguishable from their respective parental strains.

Measurements performed with isolated photosynthetic membranes (chromatophores) gave results similar to those seen with whole cells. The 500–900 ps fluorescence components are unaffected by photooxidation of reaction centers in the membrane, indicating that these components do not represent quenching of fluorescence by reaction centers. All fluorescence components had essentially identical fluorescence spectra between 890 and 940 nm, and thus all probably represented antenna fluorescence.

Discussion

This report describes the generation and analysis of interspecies *puf* operon chimeras between *Rhodobacter capsulatus* and *Rhodobacter sphaeroides* using a novel mutagenesis technique referred to as chimeric rescue. Though the construction of chimeric genes has been used in the

Table 3. Fluorescence decay analysis[a]

Sample	τ_1 (ps)	A_1	τ_2 (ps)	A_2	τ_3 (ps)	A_3
pU2922	46	0.984	660	0.009	5740	0.007
CONV	51	0.981	549	0.012	6609	0.007
5'INV	74	0.943	505	0.044	5380	0.013
Δ_p	82	0.914	517	0.078	5882	0.008
3'INV	94	0.896	712	0.092	5999	0.012
Δ_o	106	0.522	868	0.470	5141	0.008
pNJ-1	309	0.101	897	0.899	–	–

[a] The fluorescence amplitudes are normalized such that $A_1 + A_2 + A_3 = 1.0$. The experimental error in τ_1, τ_2, τ_3, A_2 and A_3 is about 10%. The value of A_1 and its error depend on A_2 and A_3 as described above. The values for each fluorescence decay parameter shown represent averages for the whole class of mutants (CONVs, 5'INVs, etc.). Within any class, decay times varied by about 10% between individual mutants, A_2 varied by 20% and A_3 varied by about 30%.

past to analyze protein function (see for example Taguchi 1986, Lamarre et al. 1989, Ogawa et al. 1992), the method described here takes advantage of the ability of homologous genes to recombine under selection in vivo. This method has accomplished several things that directed mutagenesis could not have. First, it allowed the simultaneous generation of a great number and variety of large-scale mutagenic events involving hundreds of base pairs to entire genes, and all of the resulting mutated reaction centers assembled and were capable of at least limited reaction center function. Second, sequence elements were identified in the *puf* operon with species-specific functional attributes; exchange of 3′ sequences of the *puf* operon between *Rb. sphaeroides* and *Rb. capsulatus* results in a significant impairment of fluorescence quenching in photosynthetic membranes. Finally, a series of mutants was generated which apparently affected the expression of the *Rb. sphaeroides puf* operon in *Rb. capsulatus*. These mutations are potentially valuable in identifying the structure of active promoter elements and locating the genomic loci encoding transcription factors in *Rb. capsulatus*.

Chimeric rescue results in a wide variety of mutagenic events

The parental *Rb. capsulatus* strain used for this study is a chromosomal deletion strain which harbors a plasmid, pNJ-1, containing both *Rb. capsulatus* host and *Rb. sphaeroides* donor *puf* operons. The *pufM* gene of the *Rb. capsulatus* host *puf* operon has a 43 bp deletion called ΔM1. This deletion removes a highly conserved loop of amino acids near the binding pocket of the secondary electron acceptor, quinone Q_A, in the M subunit which is seven amino acids longer than the corresponding region of the L subunit. With this region deleted, the *pufM* gene does not express an active gene product. pNJ-1 also contains *Rb. capsulatus* structural genes, *pufβ*, *pufα* and *pufL*, as well as *pufQ*, *pufX* and the downstream open reading frame, C2814. The *puf* operon sequences from *Rb. sphaeroides* included in pNJ-1 contain the structural genes *pufβ*, *pufα*, *pufL* and *pufM*, as well as *pufQ* and *pufX*, but lack the strong oxygen sensitive promoter which controls most of the transcription from the *puf* operon (Hunter et al. 1991). Thus, reaction center deletion strain U43 harboring pNJ-1 does not grow photosynthetically. Microaerobically grown cells (heterotrophically grown at low oxygen tension) do not show any spectral indication that reaction centers are present (Fig. 4) nor do time-resolved fluorescence measurements give any indication of the fast quenching of antenna fluorescence normally associated with reaction center function (Fig. 5, Table 3). In order for pNJ-1 to express the required functional gene products for photosynthetic activity, either the ΔM1 deletion in the *Rb. capsulatus pufM* gene must be repaired or the *Rb. sphaeroides* operon must be modified to produce these gene products.

The two *puf* operons present on pNJ-1 were placed adjacent to each other and oriented in opposite directions to facilitate homologous recombination events. One such event is a single cross-over event resulting in the reciprocal exchange of sequence 3′ of the recombination point in between the two operons (an inversion). Five recombinants, called INV mutants, were isolated as presumptive results of this type of reciprocal event. In all five cases, the inversion point was 5′ of the ΔM1 deletion in *Rb. capsulatus pufM* resulting in the exchange of the deleted region for intact sequence from the *Rb. sphaeroides* donor *puf* operon. The inversion points displayed some clustering with four inversion points falling between nucleotides M528 and M572 (Fig. 3, Table 2). One inversion point was located far 5′ of both *pufM* and *pufL* in the *Eco*RI–*Hin*DIII fragment which roughly delineates the *pufβ–pufα* region. This is consistent with previous work showing that the *puf* operon of *Rb. sphaeroides* can complement photosynthetic function in a *Rb. capsulatus* deletion strain lacking the *puf* operon (Zilsel et al. 1989). The 3′INVs show that partial replacement of reaction center genes which result in the formation of chimeric reaction centers also yields photosynthetic activity.

The most populous class of revertants (27 out of 44 total revertants) appeared to be the result of non-reciprocal recombination, either inter- or intraplasmid, where *Rb. sphaeroides* donor sequence was utilized to repair the ΔM1 deletion in the *Rb. capsulatus pufM* gene with no detected

alteration of *Rb. sphaeroides* donor sequences. (It is also possible that these CONV mutants were the result of interplasmid reciprocal exchange. However, this seems less likely since reciprocal exchange could be the result of a double recombination event as opposed to the single recombination event required for non-reciprocal exchange.) Like the INV mutants, the CONV mutants showed clustering of the 5′ ends of their conversion tracts (Fig. 3, Table 2). Though the ΔM1 deletion only removes 43 bp, all of the conversion tracts are at least three times that long, ranging from about 160 to 385 bp in length. Consistent with this, all of the inversion points are more than 100 bps 5′ to the beginning of the ΔM1 deletion. No inversion points or conversion endpoints were found within sequences encoding the D-helix of the M subunit and in each case, the entire D-helix and half of the D/E-interhelix was replaced with *Rb. sphaeroides* amino acid sequence. The 3′ ends of the conversion tracts were fairly evenly distributed, both in terms of position and of homology in the local region.

In Fig. 3, it is clear that high homology in the M535–M890 region is strongly correlated with clustering of inversion points and conversion endpoints; as expected, the level of homology appears to play a significant role in the frequency of recombination events. No INV endpoints or CONV tract endpoints were identified between M460 and M525; this region exhibited decreased homology to *Rb. sphaeroides pufM* sequence. However, the distribution of endpoints within the M535 to M890 region is non-random, indicating that other factors such as the reciprocal/non-reciprocal recombination systems or final reaction center functionality must play a significant role.

The recombination events observed in this study of *Rb. capsulatus* bear marked similarities to the recombination events so well studied in other systems such as the eukaryotic fungi (Esposito and Wagstaff 1981, Fogel et al. 1981) as well as maize and *Drosophila*. In yeast, statistically significant non-random correlations of reciprocal exchanges with gene conversion events in the same DNA region have been demonstrated (Esposito and Wagstaff 1981). In the *Rb. capsulatus* studies reported here, the conversion events (CONVs) are more prevalent than reciprocal exchanges (INVs) as has been repeatedly observed in yeast. Also, as in yeast, the prevalence of the CONV mutants in the work reported here indicates that conversion events are insensitive to the presence of a deletion (ΔM1) or of a large intervening region between the recombination points (*Rb. capsulatus pufX*, C2814, *Rb. sphaeroides pufX*). The CONV tract lengths are similar to those seen during meiotic gene conversion in yeast. Meiotic conversion events in yeast also display polarity with a gradient of conversion frequencies across genes. One likely hypothesis is that the non-random distribution of CONV and INV events observed in this study is the mechanistic result of the intrinsic reciprocal/non-reciprocal recombination systems of *Rb. capsulatus*. One can speculate that the heterozygosity present during chimeric rescue may even stimulate these repair processes.

A second contrasting hypothesis is suggested by a comparison of the sequence on the two sides of the ΔM1 deletion and the distribution of CONV tract endpoints; there could be a significant phenotypic difference between the *Rb. sphaeroides* and *Rb. capsulatus pufM* sequences encoding the D-helix of M or sequences just 3′ of this region which are deleted in ΔM1. This region of M in *Rb. sphaeroides* may differ from that in *Rb. capsulatus* such that a partial exchange of sequence may exhibit seriously impaired reaction center function. However, there are only three amino acid differences in this region between *Rb. capsulatus* and *Rb. sphaeroides* (M206, Ala to Phe; M225, Thr to Ser; M237, Ala to Val), making this hypothesis less likely.

Exchange of 3′ sequences in the puf *operon affects the efficiency of energy trapping*

Zilsel and coworkers (1989) performed steady state fluorimetry on photosynthetic membranes resulting from expression of the *Rb. sphaeroides puf* operon in *Rb. capsulatus* host cells and found a decreased efficiency of fluorescence quenching when compared to wild type. They speculated that the *Rb. capsulatus* H subunit of the reaction center (encoded chromosomally on

a different operon) and the *Rb. sphaeroides* L and M subunits were not perfectly compatible, assembling to form a somewhat impaired reaction center.

None of the CONV revertants described in this report showed a substantial phenotypic deviation from wild type, either in their growth rates, absorbance spectra, or fluorescence decay characteristics. This is not too surprising given the high degree of amino acid sequence homology in the region covered by the CONV events (nonidentities occur in amino acids M156–M273; helices C through E). In fact, there are only 11 amino acid differences between *Rb. capsulatus* and *Rb. sphaeroides* in this region. However, all of the INV revertants described in this report show a major increase in integrated fluorescence as was seen when the entire *Rb. sphaeroides puf* operon was expressed in *Rb. capsulatus* (Zilsel et al. 1989). More can be learned from Fig. 3 about the relationship between the fluorescence phenotype observed for the INVs and the genotype which gives rise to the increased fluorescence. Consider CONV14, CONV15, and INV1. CONV14 and CONV15 both have essentially wild type fluorescence phenotypes, while INV1 had the high fluorescence phenotype. The only sequence changes in INV1 which are not present in either CONV14 or CONV15 are those changes 3′ of M882 in the *puf* operon. This implies that the high fluorescence phenotype is either due to changes in the last 11 amino acids in M (amino acids M296–M306) or to some sequence in the *puf* operon 3′ of *pufM*.

One might be tempted to conclude that alteration of the gene just downstream of *pufM*, *pufX*, was resulting in the high fluorescence phenotype of the INV mutants. This gene is the only gene downstream of *pufM* in the *puf* operon that is known to affect photosynthetic function (Klug and Cohen 1988, Farchaus et al. 1990, Lilburn et al. 1992), and this gene is not conserved as well as are the other *puf* operon genes between species. However, when this gene is deleted, there are only relatively minor changes in the amplitudes and kinetics of the time-resolved fluorescence, much less pronounced than the fluorescence changes observed here (T. Beatty, A. Taguchi, and N. Woodbury, unpublished results). Though it is formally possible that replacement of *pufX* by *Rb. sphaeroides* sequences has a much more dramatic effect on fluorescence quenching than deletion of this gene, it seems unlikely.

A more likely possibility is that the C-terminal end of the M subunit plays a critical and very species-specific role in proper assembly and/or proper function of the reaction center-antenna complex in the photosynthetic membrane. This could be due, as suggested previously (Zilsel et al. 1989) to a species-specific interaction between M and the third reaction center subunit, H. Indeed, the C-terminal end of M does come in close contact (within 10 Å) with the transmembrane helix of the H subunit in *Rb. sphaeroides* (determined from molecular models based on the *Rb. sphaeroides* X-ray coordinates, Brookhaven data base file 1RCR and Allen et al. 1987). This would imply that one or more of the following amino acid changes gives rise to this phenotype: M296 (Ala to Gly), M298 (Val to Asn), M301 (Tyr to Met), or M304–M306 (Val Thr Pro to Leu Asn).

Finally, it is possible that exchange of 3′ sequences between the *puf* operons of *Rb. capsulatus* and *Rb. sphaeroides* results in destabilization of the *puf* mRNA(s) and changes in the relative levels of reaction center and antenna proteins.

Further characterization of deletions in the 3′ region of the *puf* operon are in progress and will hopefully distinguish between these various possibilities.

The Δ_p subclass of mutations affects the expression of Rb. sphaeroides *gene sequences in* Rb. capsulatus

One quarter of the revertants did not repair the ΔM1 deletion in the *pufM* gene of *Rb. capsulatus*, but were still able to grow photosynthetically. Mating experiments divided these mutants into two subclasses: 1) those which required only the *Rb. sphaeroides puf* operon on the isolated plasmid for photosynthetic function (Δ_p) and 2) those which required additional mutations not contained on the isolated plasmid (Δ_o). In both subclasses there were no obvious changes in restriction pattern when compared to the parental pNJ-1 plasmid and no sequence alteration

was found near the ΔM1 deletion. In the Δ_p subclass, it is likely that the mutation affected the ability of the *Rb. sphaeroides puf* operon sequences present in pNJ-1 to be expressed in *Rb. capsulatus*. It is most likely that the *Rb. sphaeroides pufβ* and *pufα* antenna genes were being utilized, but, as in the other mutants, *Rb. capsulatus* antenna genes may also have been produced since the *Rb. capsulatus* promoter was intact. The mechanism of reversion in the Δ_o subclass is unclear since its ability to restore photosynthetic activity was not due solely to either the isolated plasmid or the genome of the plasmid-cured cells.

Recently, transcriptional control of the *puf* operon has been the subject of considerable research effort as well as debate. In particular, the regulation of this operon by oxygen levels has been intensely investigated. The major promoter appears to be located about 320 bp 5′ of the *pufQ* coding sequence and is strongly regulated by oxygen levels (Bauer et al. 1988, Marrs 1990, Hunter et al. 1991). A second promoter has been identified 5′ of the *pufQ* gene which is very weak and constitutive with respect to oxygen levels. In addition, transcription initiation apparently can occur near the 5′ end of the *pufβ* gene in *Rb. sphaeroides* (Donohue et al. 1988).

The *Rb. sphaeroides puf* operon segment used in these studies included only the region 5′ of *pufQ* as far as the *Pst*I site. This is less than 300 bp upstream of *pufQ*, and thus, does not include the strong oxygen regulated promoter (Bauer et al. 1988, Hunter et al. 1991). This region does include sequence upstream of *pufβ* which has been shown to promote some transcription in cell-free extracts (Kiley et al. 1987). However, the parental plasmid in the revertant analysis described here, pNJ-1, did not show any significant amount of photosynthetic reaction center complex assembly in the optical spectrum (Fig. 4) when expressed in *Rb. capsulatus* nor any significant fluorescence quenching activity of the reaction center in the time-resolved fluorescence measurements (Fig. 5). In the Δ_p and Δ_o revertants, which retained the ΔM1 deletion in *pufM* of *Rb. capsulatus*, functional reaction centers were clearly produced. The most obvious hypothesis is that the Δ_p revertants (which carried the ability to complement photosynthetic activity on the plasmid) involve mutations in or near promoters present in the segment of the *Rb. sphaeroides puf* operon used in these studies which increased their activity in a *Rb. capsulatus* background.

Acknowledgements

The authors would like to thank Drs James Allen, JoAnn Williams, and Craig Schenck for helpful discussions. The authors also thank Dr JoAnn Williams for her sequence similarity computer program, SIM, and Min Li for her help with the curing experiments. NWW, AKWT and SGB acknowledge support from the NSF Biophysics program. NWW performed part of this work at Stanford as an NSF Plant Molecular Biology Postdoctoral Fellow. JWS was an NSF Predoctoral Fellow. This work utilized instrumentation purchased with funds from DOE instrumentation grants DE FG05 88ER75443 and DE FG05 87ER75361 (University Research Instrumentation Program). This is publication #146 from the Arizona State University Center for the Study of Early Events in Photosynthesis. The Center is funded by US Department of Energy grant DE FG02 88ER13969 as part of the USDA/DOE/NSF Plant Science Centers program.

References

Allen JP, Feher G, Yeates TO, Komiya H and Rees DC (1987) Structure of the reaction center from *Rhodobacter sphaeroides* R-26: The cofactors. Proc Natl Acad Sci USA 84: 5730–5734

Bauer CE, Young DA and Marrs BL (1988) Analysis of the *Rhodobacter capsulatus puf* operon. Location of the oxygen-regulated promoter region and the identification of an additional *puf*-encoded gene. J Biol Chem 263: 4820–4827

Biel AJ and Marrs BL (1983) Transcriptional regulation of several genes for bacteriochlorophyll biosynthesis in *Rhodopseudomonas capsulatus* in response to oxygen. J Bact 156: 686–694

Bylina EJ, Ismail S and Youvan DC (1986) Plasmid pU29, a vehicle for mutagenesis of the photosynthetic *puf* operon in *Rhodopseudomonas capsulata*. Plasmid 16: 175–181

Bylina EJ, Jovine RVM and Youvan DC (1989) A genetic system for rapidly assessing herbicides that compete for the

quinone binding-site of photosynthetic reaction centers. Bio/Technology 7: 69–74

Chang C-H, El-Kabbani O, Tiede D, Norris J and Schiffer M (1991) Structure of the membrane-bound protein photosynthetic reaction center from *Rhodobacter sphaeroides*. Biochemistry 30: 5352–5360.

Donohue TJ, Kiley PJ and Kaplan S (1988) The puf operon region of *Rhodobacter sphaeroides*. Photosynth Res 19: 39–61

Esposito MS and Wagstaff JE (1981) Mechanisms of mitotic recombination. In: Strathern JN, Jones EW and Broach JR (eds) The Molecular Biology of the Yeast Saccharomyces, Life Cycle and Inheritance, pp 341–370. Cold Spring Harbor Laboratory Press, Cold Spring Harbor

Farchaus JW, Gruenberg J, Gray KA, Wachtveitl J, Deltoff B, Kaplan S and Oesterhelt D (1990) The *puf* B, A, L, M genes are not sufficient to restore the photosynthetic plus phenotype to a *puf* L, M, X deletion strain. In: Drew G and Dawes EA (eds) Molecular Biology of Membrane-bound Complexes in Phototropic Bacteria, pp 65–75. Plenum Press, New York

Feher G, Allen JP, Okamura MY and Rees DC (1989) Structure and function of bacterial photosynthetic reaction centres. Nature 339: 111–116

Fogel S, Mortimer RK and Lusnak K (1981) Mechanisms of meiotic gene conversion, or 'wanderings on a foreign strand'. In: Strathern JN, Jones EW and Broach JR (eds) The Molecular Biology of the Yeast Saccharomyces, Life Cycle and Inheritance, pp 289–339. Cold Spring Harbor Laboratory Press, Cold Spring Harbor

Gust D, Moore TA, Luttrull DK, Seely GR, Bittersmann E, Bensasson RV, Rougee M, Land EJ, De Schryver FC and Van der Auweraer M (1990) Photophysical properties of 2-nitro-5,10,15,20-tetra-*p*-tolylporphyrins. Photochem Photobiol 51(4): 419–426

Hunter CN, McGlynn P, Ashby MK, Burgess JG and Olsen JD (1991) DNA sequencing and complementation deletion analysis of the *bchA-puf* operon region of *Rhodobacter sphaeroides*: In vivo mapping of the oxygen-regulated puf promoter. Molec Microbiol 5: 2649–2661

Kiley PJ, Donohue TJ, Havelka WA and Kaplan S (1987) DNA sequence and in vitro expression of the B875 light-harvesting polypeptides of *Rhodobacter sphaeroides*. J Bacteriol 169: 742–750

Kirmaier C and Holten D (1987) Primary photochemistry of reaction centers from the photosynthetic purple bacteria. Photosynth Res 13: 225–260

Klug G and Cohen SN (1988) Pleiotropic effects of localized *Rhodobacter capsulatus puf* operon deletions on production of light-absorbing pigment–protein complexes. J Bacteriol 170: 5814–5821

Lamarre D, Ashkenazi A, Fleury S, Smith DH, Sekaly R and Capon DJ (1989) The MHC-binding and gp120-binding functions of CD4 are separable. Science 245: 743–746

Lilburn TG, Haith CE, Prince RC and Beatty JT (1992) Pleiotropic effects of *pufX* gene mutation on the structure and function of the photosynthetic apparatus of *Rhodobacter capsulatus*. Biochim Biophys Acta 1100(2): 160

Magnin J, Willison JC and Vignais PM (1987) Elimination of R plasmids from the photosynthetic bacterium *Rhodobacter capsulatus*. FEMS Microbiol Lett 41: 157–161

Maniatis T, Fritsch EF and Sambrook J (1982) Molecular Cloning: A Laboratory Manual. Cold Spring Harbor Laboratory Press, Cold Spring Harbor

Marrs BL (1990) Molecular genetics studies of gene expression and protein structure/function relationships in photosynthetic bacteria. In: Drews G and Dawes EA (eds) Molecular Biology of Membrane-bound Complexes in Phototrophic Bacteria, pp 1–4. Plenum Press, New York

Ogawa T, Shinohara A, Ogawa H and Tomizawa J (1992) Functional structures of the RecA protein found by chimera analysis. J Mol Biol 226: 651–660

Parson WW (1991) Electron transfer in reaction centers. In: Scheer H (ed) Chlorophylls, pp 1153–1180. CRC Press, Boca Raton

Schenck CC, Blankenship RE and Parsons WW (1982) Radical-pair decay kinetics, triplet yields and delayed fluorescence from bacterial reaction centers. Biochim Biophys Acta 680: 44–59

Scolnik PA and Marrs BL (1987) Genetic research with photosynthetic bacteria. Ann Rev Microbiol 41: 703–726

Simon R, Priefer U and Puhler A (1983) A broad host range mobilization system for in vivo genetic engineering: Transposon mutagenesis in gram-negative bacteria. Bio/Technology 1: 784–791

Taguchi AK (1986) *ADR6*: A regulatory locus for the cytoplasmic alcohol dehydrogenases of *Saccharomyces cerevisiae* (thesis). Seattle: University of Washington

Taguchi AKW, Stocker JW, Alden RG, Causgrove TP, Peloquin JM, Boxer SG and Woodbury NW (1992) Biochemical characterization and electron-transfer reactions of *sym1*, a *Rhodobacter capsulatus* reaction center symmetry mutant which affects the initial electron donor. Biochemistry 31: 10345–10355

Valkunas L, Liuolia V and Freiberg A (1991) Picosecond processes in chromatophores at various excitation intensities. Photosynth Res 27: 83–95

Van Grondelle R (1985) Excitation energy transfer, trapping and annihilation in photosynthetic systems. Biochim Biophys Acta 811: 147–195

Weaver RF, Wall JD and Gest H (1975) Characterization of *Rhodopseudomonas capsulata*. Arch Microbiol 105: 207–216

Williams JC, Steiner LA, Ogden RC, Simon MI and Feher G (1983) Primary structure of the M subunit of the reaction center from *Rhodopseudomonas sphaeroides*. Proc Natl Acad Sci USA 80: 6505–6509

Williams JC, Steiner LA, Feher G and Simon MI (1984) Primary structure of the L subunit of the reaction center from *Rhodopseudomonas sphaeroides*. Proc Natl Acad Sci USA 81: 7303–7307

Woodbury NWT and Parson WW (1984) Nanosecond fluorescence from isolated photosynthetic reaction centers of *Rhodopseudomonas sphaeroides*. Biochim Biophys Acta 767: 345–361

Woodbury NW and Parson WW (1986) Nanosecond fluorescence from chromatophores of *Rhodopseudomonas sphaer-*

oides and *Rhodospirillum rubrum*. Biochim Biophys Acta 850: 197–210

Youvan DC, Bylina EJ, Alberti M, Begusch H and Hearst JE (1984) Nucleotide and deduced polypeptide sequences of the photosynthetic reaction-center, B870 antenna, and flanking polypeptides from *R. capsulata*. Cell 37: 949–957

Youvan DC, Ismail S and Bylina EJ (1985) Chromosomal deletion and plasmid complementation of the photosynthetic reaction center and light-harvesting genes from *Rhodopseudomonas capsulata*. Gene 38: 19–30

Zilsel J, Lilburn TG and Beatty JT (1989) Formation of functional inter-species hybrid photosynthetic complexes in *Rhodobacter capsulatus*. FEBS Lett 253(1,2): 247–252